# Estimating Urban Heat Island Intensity using Remote Sensing Techniques in Dhaka City

Nigar Sultana Parvin, Dan Abudu

**Abstract**—This study assessed the effects of urban heat island in Dhaka city, Bangladesh from 2002 to 2014 using remote sensing techniques. Land cover changes were characterized over a twelve year period with keen interested on urban expansion and the resulting impacts created by these changes on the land surface temperatures investigated. The study also compared the land surface temperature and ground station temperature data to validate the surface temperature in Dhaka. Maximum likelihood supervised classification method was used for the land cover classification resulting in a classification accuracy of 86.5% and 90.7% for 2002 and 2014 respectively. Remarkable change in land cover was observed in built-up areas which increased by 21% of the total land area from 74.12 to 135.36 square kilometres in 2002 and 2014 respectively. Combined end member selection and linear mixture model techniques were used to estimate the surface emissivity of the land surface properties. The obtained surface emissivity together with the brightness temperatures of the thermal bands were then used to calculate the land surface temperature. Results showed that land surface temperature increased throughout the study area. Temperature ranges of 28.5°C to 35.4°C were observed in 2002 and 37.9°C to 40.1°C in 2014. The difference between ground-based temperature and the satellite derived temperatures for the ground weather station were +1.8°C and +2.7°C in 2002 and 2014 respectively. This margin of difference is attributed to sensor calibration errors. The land surface temperature increased across all land cover types over the twelve year period indicating existence and potential effects of urban heat highland in the Dhaka city. The results indicates that there is urgent need for the city authority to implement measures that must monitor and contain the resulting effects on the city population and infrastructure.

**Index Terms**— Urban Heat Island, Remote Sensing, GIS, Land Cover Classification, LST, Linear Mixture Modelling, Dhaka, Bangladesh.

————————————— ◆ —————————————

## 1 INTRODUCTION

Dhaka city has experienced higher temperatures over the last decade depicted by hotter summer days and day-time's scorching heat coupled with load shedding [1],[2]. Several factors are considered to have contributed to this temperature increases, but one factor has been repeatedly supported by literature to have contributed to Dhaka's temperature rise; a unique phenomenon of the urban climate known as Urban Heat Island (UHI) effect [3],[4]. The UHI phenomenon was first recognised in London in the early 19th Century and since then there have been suggestions to the UHI effect contributing to climate change effects however, the relationship has still not been quantified and confirmed by any study [5],[6],[7].

There are various effects of UHI. It has the probability of direct influence on health and wellbeing of urban life. Cities normally show higher percentage of heat oriented sickness and mortality rate in comparison to rural areas [4]. Urban residents are deprived from cool relief at night time like cool relief in the rural areas because UHI's night time effect are harmful for the time of heat wave [8]. Furthermore, this type of poor air quality aggravates asthma effects and causes other respiratory related diseases. Asthma patient rate as noted by [9],[10] increased in Dhaka city during summertime, particularly in the poor communities who cannot afford air conditioner or any other cooling system for heat wave.
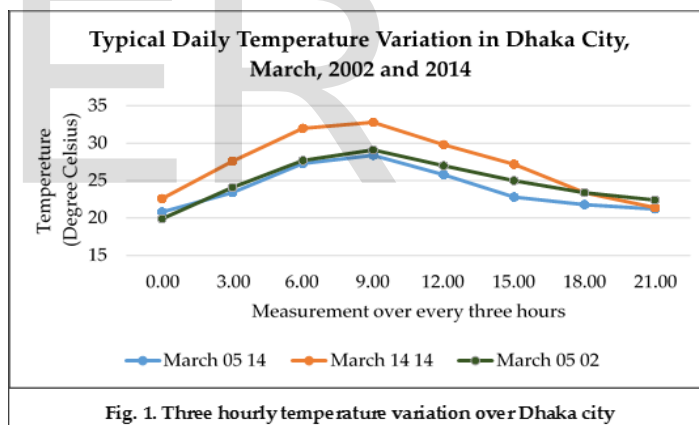


Fig. 1. Three hourly temperature variation over Dhaka city

According to the Urban Climate News [11], there is need to sensitise people on the UHI effects, carry out further studies and source funds and community support to address the effect. Cities such as Los Angeles invest over 64.9 million British pounds every year to counter the UHI effect. UHI can also affect growth of vegetation as a result of its influence on the weather. Researchers observed that plants take longer to germinate and grow properly in UHIs than in rural area [4].

Recent studies have shown that the availability of remotely sensed data covering decadal periods and earth surface has greatly led to intensified studies on relationship between land surface temperatures and land cover changes over different time periods [4],[12],[13]. These previous studies focused on land cover changes and their resulting effects on the land surface temperature, but developing cities such as Dhaka City present many opportunities for research due to its rapid population increment and urbanisation effects such as slum developments and environmental risks [4],[14]. Although the findings

————————————————
- *Nigar Sultana Parvin is currently an Assistant Director Incharge of Training at the Directorate of Secondary and Higher Education, Bangladesh. E-mail: nigarjoly@yahoo.com*
- *Dan Abudu is a Researcher and Faculty at the Department of Computer and Information Science, Muni University, Arua, Uganda. E-mail: d.abudu@muni.ac.ug*

of previous studies are important for the study area, they lack the ability to assess decadal effects of LST using uniform spatial scale imagery extending over the entire area.
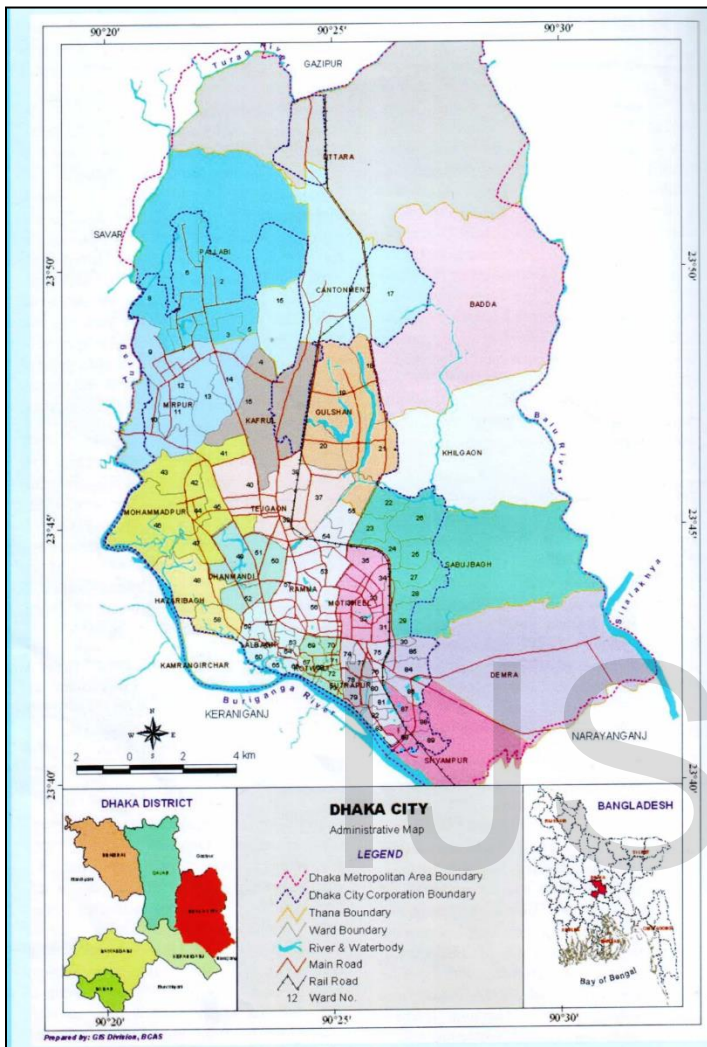


Fig. 2. Location Map of the study Area. (Source: [15])

Given that Landsat satellite programme archives satellite imagery over the study area at uniform spatial scale dating many decades back (5 decades for VIS-NIR imagery and 3 decades for SWIR and thermal), it made it possible for this study to consider a 12-year period (2002 – 2014) and investigate the impact of land cover changes on the development of UHI and its intensty in Dhaka city. The choice of the temporal periods were influenced by two factors; firstly, in the year 2014 (Fig. 1) the area experienced the highest temperature recorded in its history [16]) and secondly, in the year 2002, climatic factors were considered a factor that caused extensive outbreak of Dengue in Dhaka [8].

The study therefore, applied remote sensing techniques to estimate UHI intensity and urban expansion between 2002 and 2014. Land surface temperature and the ground measurement data were also compared in order to validate the results of the surface temperature. Finally, the relationship between temperature variation and land cover changes were determined.

Location of the study area is shown in Fig. 2. Dhaka city, the

capital of Bangladesh was awarded city status in 1610. At that time, it had a population of 30,000 persons and an areal coverage of 1.5 square kilometres. Over 100 year period, the city increased to 40 square kilometres. By the year 2013, Dhaka City Corporation, stated that the total area of Dhaka city was 1,528 square kilometres [17]. Dhaka is also Bangladesh's most densely populated city and one of the largest metropolises in South Asia. Expansion of Dhaka has been largely influenced by its elevation, higher population and economic development. The city is the headquarters of Bangladesh government for all economic and public administration.

## 2 METHODOLOGY

### 2.1 Data

The Urban Heat Island effect is embedded in a complex climatic system influenced by several factors such as land use, land cover, altitude, proximity to sea and sea breezes [18]. It is challenging to isolate the contributions of various factoring agents. Achieving the study objectives required incorporatation of multiple approaches and data such as the use of GIS and Remote Sensing techniques, ground-based temperature measurements and geostatistical analysis. The study focussed on above techniques in order to evaluate and quantify the land surface temperature (LST), examine the variation of LST over a 12-year period, and establish the relationship between LST and the different land cover types in the study area. Table 1 shows the various data used in this study.

TABLE 1
DATA AND DATA SOURCES USED IN THE STUDY

| Data | Path/ Row | Resolution | Date | Source |
|------|-----------|------------|------|--------|
| Landsat 7 ETM+ | 137/044 | 30 m | 5/3/2002 | USGS |
| Landsat 8 OLI/TIRS | 137/044 | 30 m | 14/3/2014 | USGS |
| Temperature data | | 3 hourly | 2002- 2014 | BMD |
| Roads and utility lines | | 1:100,000 | 2012 | RHD |
| Boundary | | 1:100,000 (spatial) | 2013 | RAJUK |

Landsat 7 and 8 imagery were both supplied geometrically corrected to UTM Zone 13N projection system which is consistent to the localised projection of the study area. The spatial resolution of 30 metres were mantauined across all datasets inorder to maintain geometric accuracy. Radiometric calibration were performed in ENVI software in order to derive the at-sensor data value of the imagery [19].

The temperature data were supplied in text file format which were converted to Microsoft Excel format collected on a 3-hourly interval from the Agargaon monitoring station in Dhaka over the periods of 2002 to 2014. The single station dataset is

used to collect meteorological data over Dhaka city and surrounding areas. As noted by Oke [20], two or more weather stations are required in order to understand the atmospheric condition of a large area under investigation. Given the size of Dhaka city and limited ground stations, an attempt was made to reduce the potential error margin introduced by the use of single weather station dataset by collecting datasets at a three hourly interval for the study period. Averaging were applied to the data in order to tabulate data according to day, month and year ready for analysis and comparison with LST obtained from satellite imagery.

## 2.2 Estimation of Land Cover Changes

ENVI 5.2 software tools were employed to perform classification of the Landsat images for 2002 and 2014 into four classes. The classes (Table 2) were obtained from literature review of a recent land cover classification study of the study area by Ahmed et al. [4] in order to obtain ground validation and comparison data. These classes corresponded with the derived spectral endmember used in the correction of land surface emissivity. Maximum Likelihood Supervised classification (MLC) techniques were used to perform the classification. The choice for MLC over other supervised classification techniques such as Parallelepiped and Minimum Distance techniques was due to its ability to incur reduced amount of error due to misclassification [21]. Also given that a previous study conducted in the study area by Ahmed et al. [4] applied MLC, according to Pooja et al. [22], it provides the opportunity to compare previous results with this study.

TABLE 2
CLASSES USED FOR LAND COVER CLASSIFICATION

| Classes | Description |
|---|---|
| Bareground | Fallow land, earth and sand land in-fillings, construction sites, developed land, excavation sites, open space, bare soils, and the remaining land cover types. |
| Built areas | All infrastructure—residential, commercial, mixed use and industrial areas, villages, settlements, road network, pavements, and man-made structures |
| Vegetation | Trees, natural vegetation, mixed forest, gardens, parks and playgrounds, grassland, vegetated lands, agricultural lands, and crop fields. |
| Water | River, permanent open water, lakes, ponds, canals, permanent/seasonal wetlands, low-lying areas, marshy land, and swamps |

Source: [4]

## 2.3 Linear Spectral Model and End Member Selection

There are known advantages in using endmembers for spectral unmixing processes. Firstly, they contain the same systematic errors due to atmospheric correction as the image to be unmixed. Endmembers also can represent responses from the selected material at the same scale as the original image (Roberts

et al., 1998). Endmembers were selected manually by visualising the Pixel Purity Index (PPI) results of spectrally pure pixels identified using the PPI in an N-dimensional visualiser in ENVI software. The PPI image was geographically linked to the original image to identify the image endmembers. No field trips were conducted but the land cover features were confirmed from the previous study conducted by Ahmed et al. [4] before finalising the endmember spectra. Selected endmembers were grouped into four land cover classes (Table 2). The choice for the use of this method is supported by previous study where the selection of image endmembers have been effectively performed through the use of a PPI [23].

Linear mixture Model (LMM) technique was used to perform pixel analysis to determine the relative abundance of surface materials within a pixel and as noted by Rashed et al. [24], is preferable to hard classifiers especially when dealing with medium to coarse spatial resolution satellite sensor data such as Landsat Thematic Mapper or Enhanced Thematic Plus, Moderate Resolution Imaging Spectroradiometer and Advanced Very High Resolution Radiometer.

The mathematical model used in the LMM is expressed in Equation (1). This model uses the assumption described by Adams et al. [25], where the spectrum measured by a sensor is assumed to be a linear combination of the spectra of all components within the pixel

$$R_i = \sum_{k=1}^{n} f_k R_{ik} + \varepsilon_i \quad \text{............................................... (1)}$$

Where $i$ is the number of bands (minimum = 1), $R_i$ the spectral pixel reflectance of each band ($i$), $k$ is the number of classification endmembers with a minimum of one endmember. $f_k$ is the proportion of endmember $k$ within the pixel; $R_{ik}$ is the spectral reflectance of endmember $k$ within the pixel on band $i$, and $\varepsilon_i$ is the error for band $i$. For a constrained unmixture solution, $f_k$ is subject to restrictions between zero and one (Equation (2)). The model's fit is assessed by computing the Root Mean Square Error (RMS) using the Equation (3).

$$\sum_{k=1}^{n} f_k = 1; \; for \; 0 \le f_k \le 1 \quad \text{............................................. (2)}$$

$$RMS = \sqrt{\left(\sum_{i=1}^{n} (\varepsilon_i^2)/n\right)} \quad \text{............................................. (3)}$$

Calculation of the RMS is done for all the image pixels. Attaining low RMS values signify better fit of the model [26]. Therefore, accuracy of the endmember selection and the sufficiency of the selected number can be assessed for accuracy by analysing the error image. Similarly, attaining quality fraction images is greatly influenced by the number of endmembers selected and the proper purity of the selected endmembers. A bad endmember selection and identification can lead to meaningless fraction cover maps.

The endmembers selected for this study were then used for Linear Spectral Unmixing (LSU). LSU assumes that; (i) spectral variation is caused by a limited number of surface materials (i.e. soil, water, shadow, vegetation), (ii) the pixel is a linear mixture of its constituents and (iii) all endmembers possibly contained in the pixel have been included in the analysis [27]. During the

unmixing process, a unit sum constraint was applied by adding a weighting factor of one because the sum of abundances is theoretically one. This is the default unmixing algorithm. Fig. 3 shows the summary of the methodology.



Fig. 3. Methodological Flow Diagram
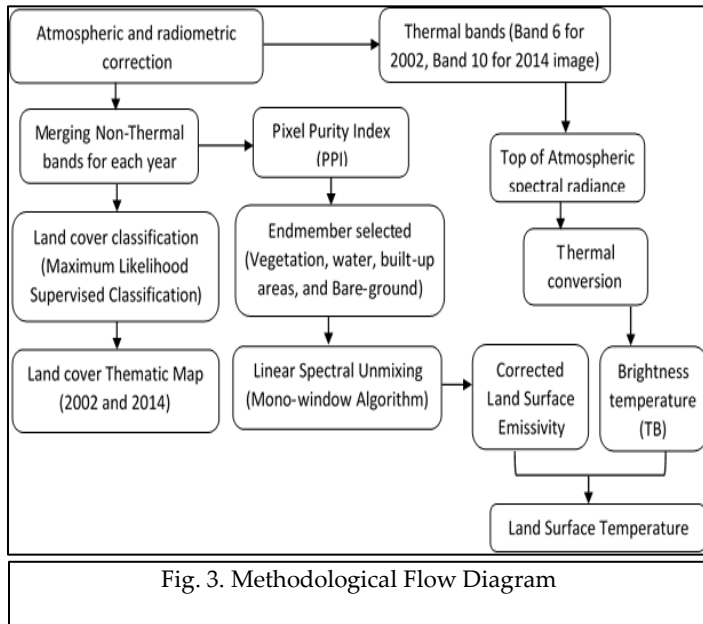
## 2.4  Calculation of Land Surface Temperature (LST)

The surface radiant temperature were derived from geometrically corrected Landsat ETM+ thermal infrared (TIR) band 6 and Landsat 8 Thermal Infrared Sensor (TIRS) bands 10 and 11. Bands 10 and 11 of the Landsat 8 TIRS records thermal radiation in spectral range of 10.60 - 11.19 and 11.50 - 12.51 μm respectively. While the ETM+ Band 6 records with spectral range of 10.4 - 12.5 μm from the earth surface.

Given that is necessary to address the effects of diurnal heating cycle on land surface temperatures, this study did not attempt to address it because OLI/TIRS and ETM+ imagery do not provide day and night infrared images on the same day, with night time overpass recorded on a different day. This attributed to the fact that the study could not analyse the variability of LST with respect to the overpass time and the years considered. The study further performed atmospheric correction in order to minimise the errors attributed to atmospheric effects (haze) and the potential of estimating inaccurate LSTs.

Estimation of LSTs follow two-step operations when extracting LSTs from satellite imagery [28]. The spectral radiance must be converted to at-sensor brightness temperature and the spectral emissivity must be corrected [29]. This study adopted the method where known emissivity values (Table 3) were used to assign pure pixels of each end member in order to correct the spectral emissivity [30].  Then the calculation of corrected LST performed based on the Equation (4) proposed by Weng and Yang [31].

$$LST = \left( \frac{TB}{1+(\lambda * TB / \text{p})\, ln\, LSE} \right) \dots\dots\dots\dots\dots\dots\dots\dots\dots\dots\dots\dots\dots\dots\dots \quad (4)$$

Where, LST = Land Surface Temperature in Kelvin; TB = brightness temperature of thermal bands (band 6 for ETM+ and 10 for TIRS) in kelvin; LSE = Corrected Land Surface Emissivity values (Table 4 used in the calculations); λ = wavelength of emitted radiance (Table 3); p = h * c/f (1.439 x $10^{-2}$ m K) where f = Boltzmann's constant (1.38 x $10^{-23}$ J/K), h = Planck's constant (6.626 x $10^{-34}$ J s), and c = velocity of light (2.998 x $10^{8}$ m/s).

TABLE 3

CENTRE WAVELENGTH OF THE THERMAL BANDS

| Satellite | Band | Centre wavelength (μm) |
|---|---|---|
| Landsat 4,5, 7 & ETM+ | 6 | 11.45 |
| Landsat 8 | 10 | 10.8 |
| Landsat 8 | 11 | 12 |

Source; [32],[33]

TABLE 4

EMISSIVITY VALUES OF COMMON LAND COVER TYPES

| Land cover type | Emissivity (ε) |
|---|---|
| Bare ground (soil) | 0.93 |
| Vegetation (Grass) | 0.98 |
| Built-up (Concrete) | 0.94 |
| Water | 0.97 |

Source; [34]

The ENVI's band math formula is given by:
TB / (1 + (10.8 * TB / 14380) * log (ε)) requiring the values of surface emissivity for the land cover types under consideration and the brightness temperature.

### 2.4.1    Land Surface Emissivity (LSE)

The temperature values for constants used in Equation (4) are defined in temperature measurement units of Kelvin. These temperature values were obtained referenced to absolute temperature of a black body, rather than the land cover types of the study area. Therefore, it is imperative to perform LSE corrections that are specific to the different land cover types. Emissivity values specific to each land cover type are listed in Table 4 according to the classification scheme proposed by Snyder et al. [30].

Equation (5) is used to correct the LSE for specific land cover class and it considers that LSE depends on the composition, structure, wetness and observation conditions of the surface [35]. Therefore, considering there are N kinds of endmembers in a pixel, and the temperature of all endmembers are the same, the relationship between endmember fraction and the corrected emissivity (LSE) in the pixel is proportional [36],[37].

$$LSE = \left( \sum_{i=1}^{N} \varepsilon i * fi \right) \dots\dots\dots\dots\dots\dots\dots\dots\dots\dots\dots\dots\dots\dots\dots\dots\dots \quad (5)$$

Where, εi is emissivity of endmember i, fi is the fraction of endmember i in a pixel.

The corrected LSE are then applied to Equation (4) to obtain the corrected LST.

### 2.4.2    Brightness Temperature (TB)

Brightness temperature (TB) is the microwave radiation radiance traveling upward from the top of Earth's atmosphere.

The calibration process has been done for converting thermal DN values of thermal bands of TIR to TB. For finding TB of an area the Top of Atmospheric (TOA) spectral radiance (R) is required. TB for both the TIRs bands was calculated by using the formula in Equation (5):

$$TB = \frac{K2}{(ln(\frac{K1}{R}+1))} \dots\dots\dots\dots\dots\dots\dots\dots\dots\dots\dots\dots\dots\dots\dots (6)$$

Where, K1 and K2 are the thermal conversion constant and it varies for both TIR bands (Table 5), and R is the Top of Atmospheric spectral radiance (Equation (7)). The Band math equations are: K2 / log (K1 / float (Bn)) +1 where Bn is the TOA spectral radiance (R) for bands 6(2) for Landsat 7 ETM+ and band 10 for the Landsat 8 OLI/TIRS.

$$R = M_L * QCAL + A_L \dots\dots\dots\dots\dots\dots\dots\dots\dots\dots\dots\dots\dots (7)$$

Where; QCAL is the respective band 6 and 10 imagery.

TABLE 5
THERMAL CONVERSION CONSTANT AND RESCALING FACTOR FOR LANDSAT 7 ETM+ AND 8 OLI/TIRS

| | K1 | K2 | Multiplicative Rescaling Factor, $M_L$ | Additive Rescaling Factor, $A_L$ |
|---|---|---|---|---|
| Band 6 (ETM+) | 666.09 | 1282.71 | 0.067 | 0.1 |
| Band 10 (TIRS) | 777.89 | 1321.08 | 0.0003342 | 0.1 |
| Band 11 (TIRS) | 480.89 | 1201.14 | 0.0003342 | 0.1 |

Source;[38],[32]

## 2.5 Classification of Heat Zones in degrees Celsius

The obtained LST temperature values in degrees kelvin were converted to degrees Celsius using the Equation (8).

$$C = LST - 273.15 \dots\dots\dots\dots\dots\dots\dots\dots\dots\dots\dots\dots\dots\dots\dots (8)$$

The ENVI formula in Band Math for both 2002 and 2014 LST scenes was given by: (float (B1) - 1) where B1 is the corrected Land Surface Temperature image obtained in Kelvin.

## 2.6 Relationship between Land Cover Types and LST

Studies have shown that quantifying the effects of LST and its spatial patterns require proper understanding pf the relationship the LST has with specific land cover types [31]. In some cases, each of the land cover types can be considered while classifying the land cover types into vegetated and non-vegetated is as well sufficient to derive the relationship existing between land cover types and LST [39],[40]. This study extracted the minimum and maximum LST values for each of the four land cover types classified and presented average LST of each land cover types for 2002 and 2014.

## 2.7 Accuracy Assessment

A common method for accuracy assessment of a classified land cover map is through the use of an error matrix. Some important measures, such as overall accuracy, producer's accuracy, and user's accuracy, can be calculated form the error matrix [41],[42],[43]. This study used a reference random selection of 1000 pixels for each year (2002 and 2014). The sample points selected were made of features such as intersections between roads, religious monuments and landmarks. The ground validation data were obtained from a similar land cover classification of the same study area conducted Ahmed et al. [4] covering the years 1989, 1999 and 2009, and the use of Google Earth imagery. The motivation to use results from this study rather than travel to the study area was due to financial constraints and the small time frame for this study. Because of difference in the year of classification between this study's data (2002 and 2014) and the referenced land cover map (Most recent, 2009), a careful check of each sample points on the Google Earth image were conducted and the results reported in the accuracy assessment were confirmed to exist in the two images.

The overall accuracy of the classified images and the respective user's and producer's accuracy are reported in Tables 8 and 9. The user's accuracy measures the proportion of each land cover class, which is correct whereas producer's accuracy measures the proportion of the land base, which is correctly classified.

## 3 RESULTS AND DISCUSSION

### 3.1 Land Cover Classification

Fig. 4 and 6 show the fractional images representing the four land cover classes (water, vegetation, built-up areas and bare-ground) of 2002 and 2014 that were effectively extracted by applying Linear Mixture Modelling (LMM) for feature identification. Application of maximum likelihood supervised classification on the non-thermal bands of the two imagery (2002 and 2014) resulted in the thematic maps shown in Fig. 5 and a percentage land cover proportion sumarised in Fig. 3, for the time periods of 2002 and 2014.
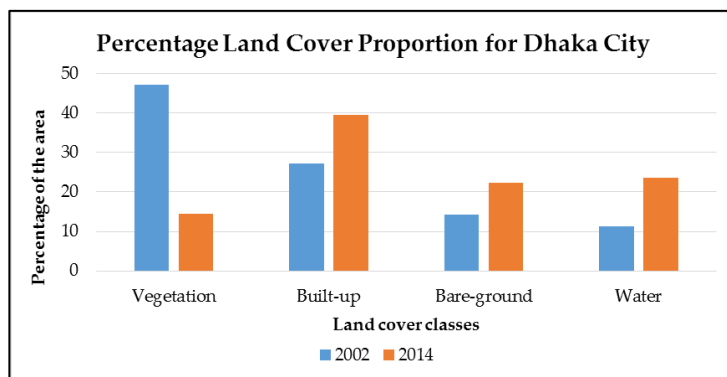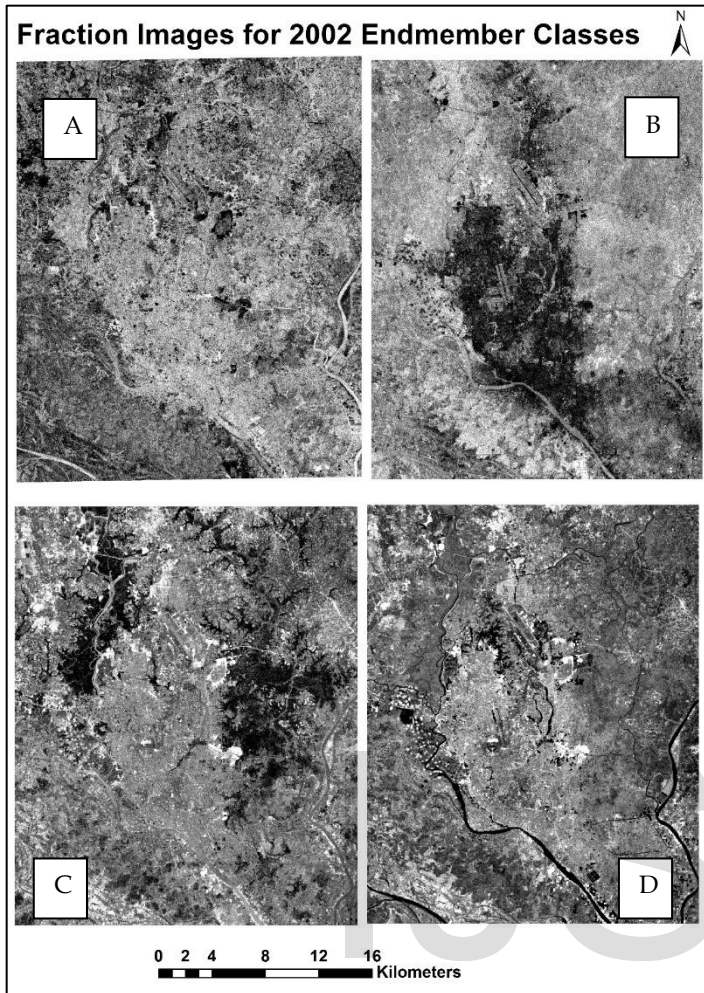


Fig. 3. 2002 and 2014 percentage land cover proportion

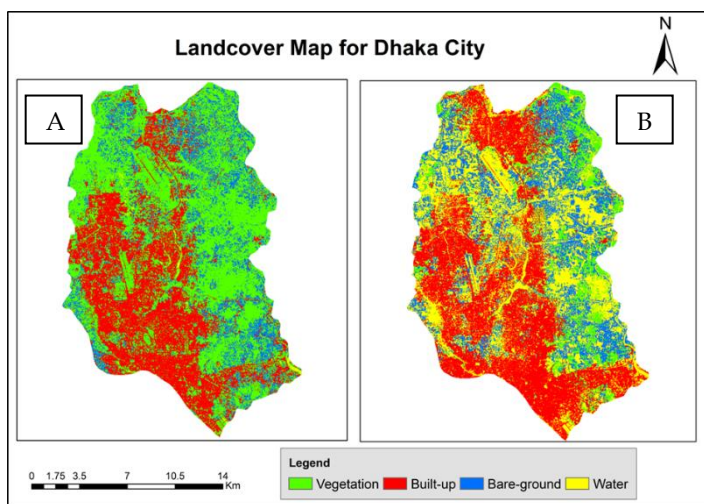Fig. 4. 2002 Fraction images for components (A) Bare-ground, B) Built-up, (C) Vegetation, (D) Water



Fig.5. Land cover change map for Dhaka from 2002 (A) to 2014 (B)

TABLE 6
AREAL (KM²) LAND COVER COVERAGE IN 2002 AND 2014

|  | Vegetation | Built-up | Bare-ground | Water |
|---|---|---|---|---|
| 2002 | 158.23 | 74.12 | 48.12 | 11.17 |
| 2014 | 52.27 | 135.36 | 64.97 | 39.04 |
| Areal Change Gain (+) & Loss(-) | -105.96 | +61.24 | +16.85 | +27.87 |
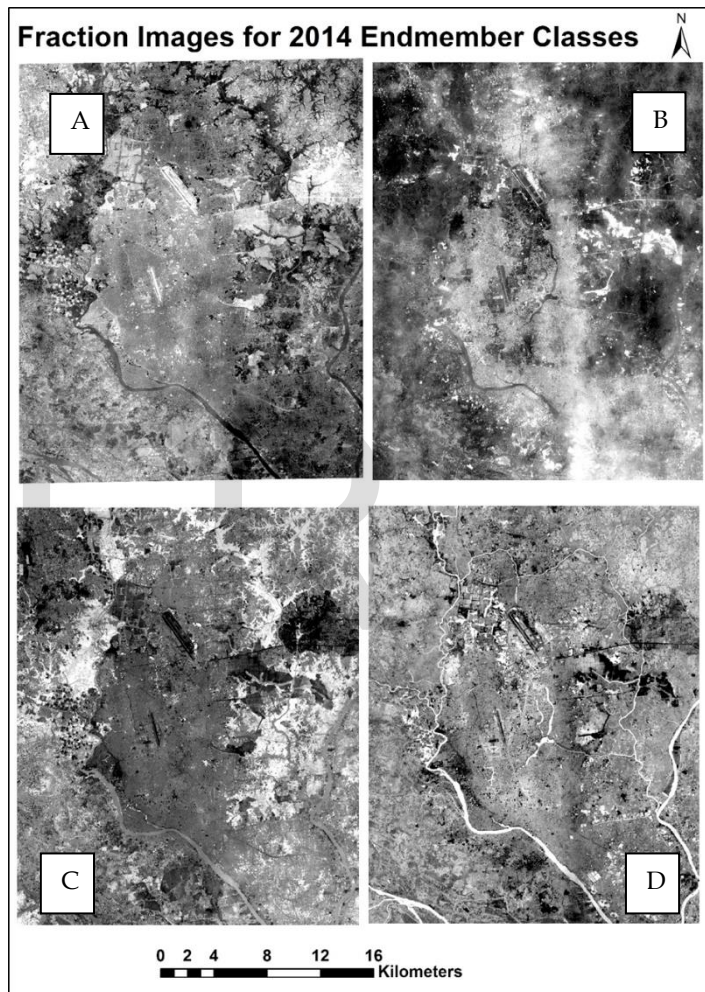


Fig.6. 2014 Fraction images for components (A) Bare-ground, (B) Built-up, (C) Vegetation, (D) Water

The result obtained from the land cover classification confirms the growth of Dhaka city as observed by previous authors [2]. Remarkable change in land cover was observed in built-up areas which increased by 21% of the total land area from 25.41% in 2002. Vegetation land cover were worst affected loosing 105.96 square kilometres to other land cover types. Similar observation was also made on water land cover type which increased by 10.7%. After evaluating Google Imagery and local knowledge of the area, in 2002 over 20% of the vegetation cover in the study area were in swampy and wetland areas. As result of urban expansion, vegetation are cleared and water surfaces

exposed.

## 3.2 Land Surface Temperatures (LST)

Two temporal time periods of 2002 and 2014 were considered for the LST change detection. Fig. 10 shows the LST change map for 2002 and 2014 respectively. The emissivity map and brightness temperature maps used to determine the LST map is shown in Fig. 7 and Fig. 8 respectively.
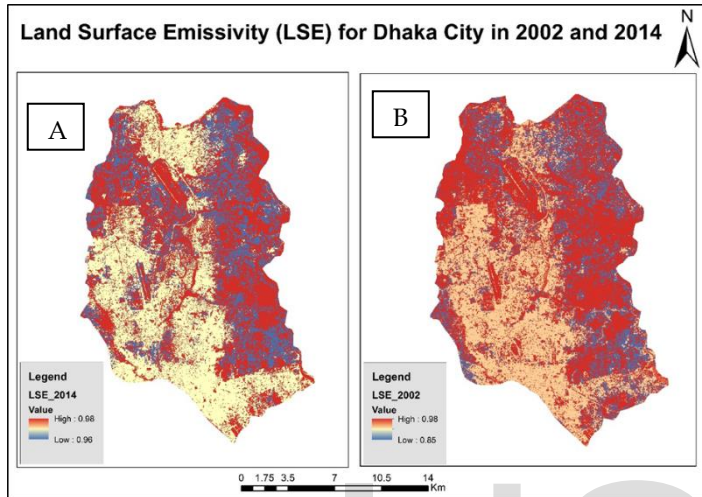


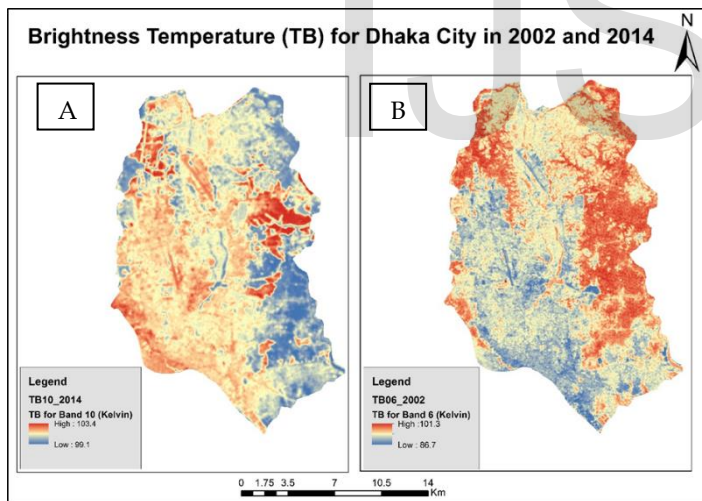Fig. 7. 2014(A) and 2002(B) Land Surface Emissivity Map of Dhaka City



Fig. 8. 2014(A) and 2002(B) Brightness Temperature Map of Dhaka City
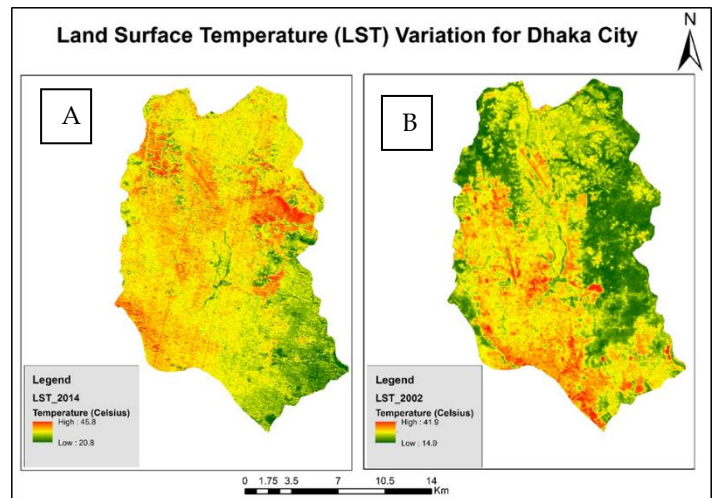




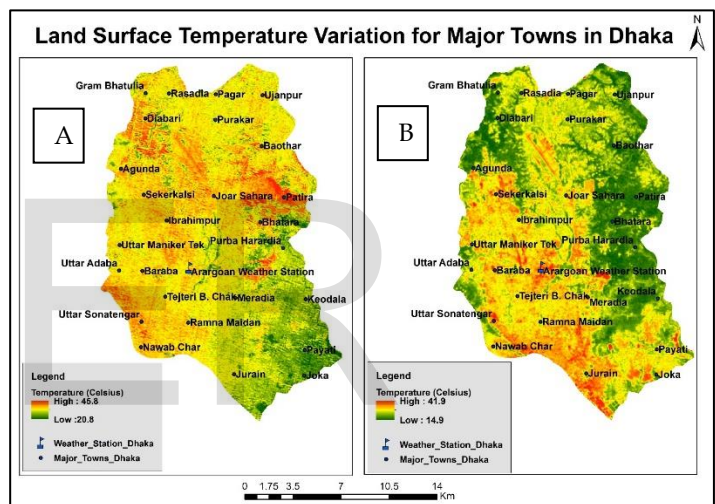Fig. 9. Land Surface Temperature changes in Dhaka City from 2014 (A) to 2002 (B)



Fig.10. LST changes for major towns in Dhaka City from 2014 (A) to 2002 (B)

Fig. 10. LST variation for each land cover class in Dhaka City

## 3.3 Temperature Variation Using Ground Station Data

The ground-based data obtained from Agargaon meteorological monitoring station in Dhaka were processd and the results shown in Fig. 11 and Fig. 12. Table 7 shows the satellite derived LST values against the ground-based LST for the single weather station and major towns in Dhaka.
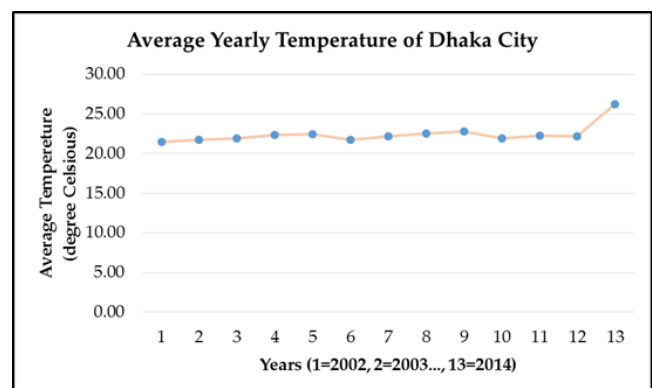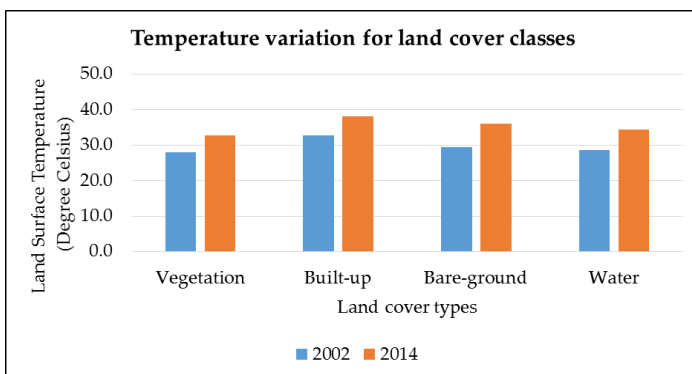
Fig.11. Average yearly temperature in degree Celsius over a 12-year period

### 3.4 Results of Accuracy Assessment

TABLE 7
SUMMARY OF THE SATELLITE DERIVED AND GROUND BASED LST VALUES FOR MAJOR TOWNS OF DHAKA

| Weather Station & Major Towns | Land Surface Temperature (degree Celsius) | | | |
|---|---|---|---|---|
| | Satellite derived | | Ground based | |
| | 05/3/2002 at 10:13am local time (GMT+6) | 14/3/2014 at 10:25am local time (GMT+6) | 05/3/2002 at 09:00am local time (GMT+6) | 14/3/2014 at 09:00am local time (GMT+6) |
| Agunda | 25.4 | 35.7 | | |
| Arargaon Station | 30.3 | 36.3 | 28.2 | 33.6 |
| Baothar | 28.3 | 37.8 | | |
| Baraba | 31.1 | 34.7 | | |
| Bhatara | 25.4 | 37.8 | | |
| Diabari | 26.3 | 37.5 | | |
| Gram Bhatulia | 26.3 | 34.9 | | |
| Ibrahimpur | 30.0 | 35.1 | | |
| Joar Sahara | 31.1 | 36.2 | | |
| Joka | 26.3 | 29.2 | | |
| Jurain | 31.1 | 31.6 | | |
| Keodala | 27.2 | 30.0 | | |
| Meradia | 31.9 | 32.7 | | |
| Nawab Char | 30.5 | 44.8 | | |
| Pagar | 28.3 | 34.3 | | |
| Patira | 26.0 | 40.1 | | |
| Payati | 30.8 | 31.3 | | |
| Purakar | 28.0 | 34.1 | | |
| Purba Harardia | 26.6 | 28.9 | | |
| Ramna Maidan | 30.8 | 35.3 | | |
| Rasadia | 26.6 | 33.3 | | |
| Sekerkalsi | 38.3 | 35.8 | | |
| Tejteri Bazar Chak | 41.1 | 44.5 | | |
| Ujanpur | 29.7 | 32.8 | | |
| Uttar Adaba | 31.0 | 32.8 | | |
| Uttar Maniker Tek | 30.2 | 35.5 | | |
| Uttar Sonatengar | 36.9 | 40.4 | | |

TABLE 8
2002 LAND COVER CLASSIFICATION ACCURACY ASSESSMENT

| | | Classified Image (2002) | | | | |
|---|---|---|---|---|---|---|
| | | Water | Vegetation | Built-up | Bare-ground | Total |
| Reference Image | Water | 218 | 18 | 4 | 10 | 250 |
| | Vegetation | 3 | 211 | 26 | 10 | 250 |
| | Built-up | 0 | 4 | 221 | 25 | 250 |
| | Bare-ground | 8 | 12 | 15 | 215 | 250 |
| | Total | 229 | 245 | 266 | 260 | 865 |
| | Producers Accuracy | 0.87 | 0.84 | 0.88 | 0.86 | |
| | Omission Error | 0.13 | 0.16 | 0.12 | 0.14 | |
| | Consumers Accuracy | 0.95 | 0.86 | 0.83 | 0.83 | |
| | Commission Error | 0.05 | 0.14 | 0.17 | 0.17 | |
| | Overall Accuracy (%): | 86.50 | | | | |
| | Average omission error (%): | 10.80 | | | | |
| | Average commission error (%): | 10.58 | | | | |

TABLE 9
2014 LAND COVER CLASSIFICATION ACCURACY ASSESSMENT

| | | Classified Image (2014) | | | | |
|---|---|---|---|---|---|---|
| | | Water | Vegetation | Built-up areas | Bare-ground | Total |
| Reference Image | Water | 208 | 18 | 12 | 12 | 250 |
| | Vegetation | 7 | 219 | 13 | 11 | 250 |
| | Built-up | 0 | 8 | 234 | 8 | 250 |
| | Bare-ground | 1 | 1 | 2 | 246 | 250 |
| | Total | 216 | 246 | 261 | 277 | 907 |
| | Producers Accuracy | 0.83 | 0.88 | 0.94 | 0.98 | |
| | Omission Error | 0.17 | 0.12 | 0.06 | 0.02 | |
| | Consumers Accuracy | 0.96 | 0.89 | 0.90 | 0.89 | |
| | Commission Error | 0.04 | 0.11 | 0.10 | 0.11 | |
| | Overall Accuracy (%): | 90.70 | | | | |
| | Average omission error (%): | 7.44 | | | | |
| | Average commission error (%): | 7.24 | | | | |
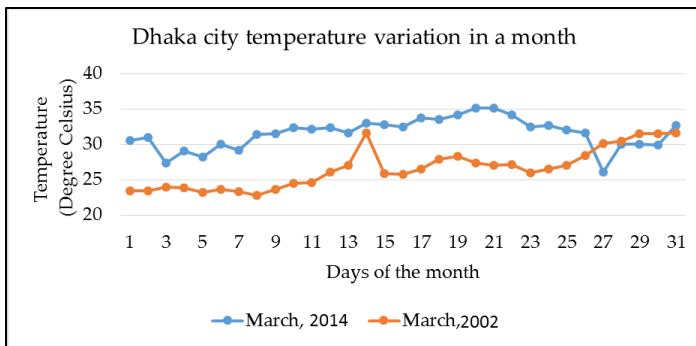
Fig.12.Temperature Variation over Dhaka city in March, 2002 and 2014

## 4 CONCLUSION

In this study, derivation of Land Surface Temperature (LST) from both Landsat 7 ETM+ and Landsat 8 OLI/TIRS were demonstrated for Dhaka City. A comparison was derived between ground-based LST and LST derived from satellite imagery. In carrying out the analyses, the following were observations were made; (i) the total area covered by built-up area increased by 61.24 square kilometres over a twelve year period from the 74.12 square kilometres observed in 2002. This increment is expected to continue over the next decade with increase in vegetation loss, (ii) Comparison between the satellite-derived LST and LST from ground measurement data, indicated that there is a gradual shift of urban centres from cooler vegetative cover in 2002 to warmer built-up areas in 2014 thereby requiring effective plans such as urban greening to curb the heating effects, and (iii) finally, the relationship between temperatures variation with land cover showed temperature increase across all land cover types in the two periods indicating significant UHI effect in the Dhaka city.

Furthermore, in this study the performance of LMM for correcting LSE for different pixels of land cover types was successfully demonstrated. It has also been shown that common concepts of urban growth and expansion have a high impact on vegetation cover and inreased UHI intensity. It is recommended that Dhaka city authority incorporate UHI countermeasure in all aspects of urban development and put in place measures to manage the resulting effects on environment and people.

## REFERENCES

[1] D.R. Raja, "Spatial Analysis of Land Surface Temperature in Dhaka Metropolitan Area," *Journal of Bangladesh Institute of Planners*, vol. 5, pp. 151-167, 2012.

[2] S. Islam, "Blazing Dhaka: An urban heat island," *The Daily Star Newspaper*, Available online at: http://ar-chive.thedailystar.net/newDesign/story.php?nid=60166, 2008.

[3] A. Rajeshwari and N.D. Mani, "Estimation of Land Surface Temperature of Dindigul District using Landsat 8 Data," *International Journal of Research in Engineering and Technology*, vol. 03, no. 05, pp. 122-126., 2014.

[4] A. Ahmed, M.D. Kamruzzaman, X. Zhu, M.D.S. Rahman, and K. Choi, "Simulating Land Cover Changes and Their Impacts on Land Surface Temperature in Dhaka, Bangladesh," *Remote Sensing,* vol. 5, pp. 5969-5998, 2013.

[5] P.D. Jones and D.H. Lister, "The urban heat island in Central London and urban-related warming trends in Central London since 1900," *Weather*, vol. 64, no. 12, pp. 323-327, 2009.

[6] P.D. Jones, D.H. Lister, and Q Li, "Urbanization effects in large-scale temperature records, with an emphasis on China," *Journal of Geophysical Research,* vol. 113, D16122, doi:10.1029/2008/JD009916, 2008.

[7] L. Howard, "The Climate of London Deduced from Meteorological Observations Made at Different Places in the Neighbourhood of the Metropolis," London: W. Phillips, George Yard, Lombard Street, 1820.

[8] M.N. Karim, S.U. Munshi, N. Anwar, and M.S. Alam, "Climatic factors influencing dengue cases in Dhaka city: A model for dengue prediction," *Indian Journal of Medical Research*, vol. 136, pp.32–39, 2012.

[9] DoE, "Assessment of the Impact of Air Pollution among School Children in Selected Schools of Dhaka City Bangladesh," Available online at: http://www.doe.gov.bd/publication_images/61_impact_of_air_pollution.pdf, 2008.

[10] G.D. Thurston, M. Lippmann, M.B. Scott, and J.M. Fine, "summertime haze air pollution and children with asthma," *American Journal of Respiratory and Critical Care Medicine*, vol. 155, no. 2, pp.654-60, 1997.

[11] Urban Climate News, "European UHI Project Targets Strategies for Heat Island Mitigation and Adaptation," available online at: http://urban-climate.org/newsletters/IAUC043.pdf, 2012.

[12] L. Liu and Y. Zhang, "Urban heat island analysis using the Landsat TM data and ASTER data: A Case study in Hong Kong," *Remote Sensing*, vol. 3, pp. 1535–1552, 2011.

[13] H. Ye, K. Wang, S. Huang, F. Chen, Y. Xiong, and X. Zhao, "Urbanisation effects on summer habitat comfort: A case study of three coastal cities in southeast China," *International Journal of Sustainable Development and World Ecology*, vol. 17, pp. 317–323, 2010.

[14] J.A. Patz, D.C. Lendrum, T. Holloway, and J.A. Foley, "Impact of regional climate change on human health," *Nature*, vol. 438, pp. 310-317, 2005.

[15] BCAS, "Climate Change Implications for Dhaka City: A Need for Immediate Measures to Reduce Vulnerability," *Resilient Cities, Local Sustainability*, vol. 1, pp 531-541, 2011.

[16] BMD, "Weather Chart," Available online at: http://www.bmd.gov.bd/?/p/=Weather-Charts, 2014.

[17] RAJUK, "Detailed Area Plan DAP". Available online at: http://www.rajukdhaka.gov.bd/rajuk/dapHome, 2013.

[18] T. Hung, U. Diasuke, O. Shiro, and Y. Yoshifumi, "Assessment with satellite data of the urban heat island effects in Asian mega cities," *International Journal of Applied Earth Observation and Geoinformation*, vol. 8, no. 1, pp.34-48, 2006.

[19] ENVI, "Radiometric Calibration," *Exelis Visual Information Solution*. Available online at: http://www.exelisvis.com/docs/RadiometricCalibration.html., 2015.

[20] T.R. Oke, "Initial guidance to obtain representative meteorological observations at urban sites," Available online at http://www.wmo.int/web/www/imop/publications-iom-series.html, 2006.

[21] D. Lu and Q.H. Weng, "A survey of image classification methods and techniques for improving classification performance," *International Journal of Remote Sensing*, vol. 28, pp.823–870, 2007.

[22] K. Pooja, S. Sonam, and A. Sonu, "A survey on image classification approaches and techniques," *International Journal of Advanced Research in Computer and Communication Engineering*, vol. 2, pp.9-12, 2013.

[23] D.A. Roberts, M. Gardner, R. Church, S. Ustin, G. Scheer, and R.O. Green, "Mapping Chaparral in the Santa Monica Mountains using multiple endmember spectral mixture models," *Remote Sensing of Environment*, vol. 65, pp.267–279, 1998.

[24] T. Rashed, J. Weeks, D. Roberts, J. Rogan, and R. Powell, "Measuring the physical compositions of urban morphology using multiple endmember spectral mixture models," *Photogrammetric Engineering & Remote Sensing*, vol. 69, no. 9, pp.1011–1020, 2003.

[25] J.B. Adams, D.E. Sabol, V. Kapos, R.A. Filho, D.A. Roberts, M.O Smith, and A.R., Gillespie, "Classification of multispectral images based on fractions of endmembers: Application to land-cover change in the Brazilian Amazon," *Remote Sensing of Environment*, vol. 52, pp. 137–154, 1995.

[26] P.M. Mather, "Computer Processing of Remotely-Sensed Images," John Wiley and Sons, England, pp 203-248, 2005.

[27] K.D. Kanniah, N.S. Wai, A.L. Meng, and A.W. Rasib, "Linear Mixture Modelling Applied to IKONOS data for mangrove mapping," Avaialble online at: http://www.a-a-r-s.org/acrs/proceeding/ACRS2005/Papers/FRR2-2.pdf, 2001.

[28] T. Blaschke, S. Lang, E. Lorup, J. Strobl, and P. Zeil, "Object Oriented Image Processing in an Integrated GIS\Remote Sensing Environment and Perspectives for Environmental Applications," *ZGIS , Zentrum Fur Geographische Informationsverarbeitung, Department of Geography and Geoinformation, University of Salzburg,* pp. 555-570, 2006.

[29] D. Lu and Q. Weng, "Spectral mixture analysis of ASTER images for examining the relationship between urban thermal features and biophysical descriptors in Indianapolis, Indiana, USA," *Remote Sensing of Environment*, vol. 104, pp. 157–167, 2006.

[30] W.C. Snyder, Z. Wan, Y. Zhang, and Y.Z. Feng, "Classification-based emissivity for land surface temperature measurement from space," *International Journal of Remote Sensing*, vol. 19, pp. 2753–2774, 1998.

[31] Q.H. Weng and S. Yang, "Managing the adverse thermal effects of urban development in a densely populated Chinese city," *Journal of Environmental Management,* vol. 70, pp.145–156, 2004.

[32] NASA, "Landsat 7 Science Data Users Handbook," National Aeronautics and Space Administration, Landsat Project Science Office at NASA's Goddard Space Flight Center: Greenbelt, MD, USA, pp. 117–120, 2010

[33] B.L. Markham and J.K. Barker, "Spectral characteristics of the LANDSAT Thematic Mapper sensors," *International Journal of Remote Sensing*, vol. 6, pp. 697 – 716, 1985.

[34] J. Mallick, C.K. Sing, S. Shashtri, A. Rahman, and S. Mukherjee, "Land Surface Emisivity retrieval based on Landsat TM satellite data over heterogeneous surfaces of Delhi city," *International Journal of Applied Earth Observation and Geoinformation*, vol. 19, pp.348-358, 2012.

[35] J. Dozzier and S.G. Warren, "Effect of viewing angle on the infrared brightness temperature of snow," *Water Resource Research*, vol. 18, pp.1424-1434, 1982.

[36] G. Tian, "Thermal Remote Sensing," Publishing House of Electronics Industry. Beijing, China, 2006.

[37] L.F. Chen, J.L. Zhuang, X.R. Xu, Z. Niu, R.H. Zhang, and Y.Q. Xiang, "The definition and validation of nonisothermal surface's effective emissivity," *Chinese Science Bulletin*, vol. 45, no. 1, pp. 22-29, 2000.

[38] D. Skokovic, J.A. Sobrino, J.C. Jimenez-Munoz, G. Soria, Y. Julien, C. Mattar, and J. Cristobal, "Calibration and Validation of Land Surface Temperature for Landsat 8 – TIRS Sensor," Land product Validation and Evolution, ESA/ESRIN Frascati (Italy), pp 6-9, 2014.

[39] J.P. Walawender, S. Mariusz, J.H. Monika, and B. Anita, "Land surface temperature patterns in the urban agglomeration of krakow, poland derived from Landsat-7/ETM+ data," *Pure and Applied Geophysics*, vol. 171, pp. 913-940, 2014.

[40] J.P. Connors, S.G. Christopher, and T.L.C. Winston, "Landscape configuration and urban heat island effects: assessing the relationship between landscape characteristics and land surface temperature in Phoenix, Arizona. *Landscape Ecology*, vol. 28, pp. 271–283, 2013.

[41] D. Abudu and M. Williams, "GIS-based optimal route selection for oil and gas pipelines in Uganda," *Advances in Computer Science: an International Journal*, vol. 4, no. 4, pp. 93-104, 2015.

[42] G.M. Foody, "Status of land cover classification accuracy assessment," *Remote Sensing of Environment,* vol. 80, pp. 185–201, 2002.

[43] P.C. Smits, S.G. Dellepiane, and R.A. Schowengerdt, "Quality assessment of image classification algorithms for land-cover mapping: A review and a proposal for a cost-based approach," *International Journal of Remote Sensing*, vol. 20, pp. 1461–1486, 1999.